Solar Physics (2022) 297:112

Temporal and Periodic Variations of the Solar Flare Index During the Last Four Solar Cycles and Their Association with Selected Geomagnetic-Activity Parameters

Atila Ozguc, Ali Kilcik, Vasyl Yurchyshyn

THE SUN, SPACE WEATHER AND GEOSPHERE Baku, Azerbaijan 1 November 2022

OUTLINE

DATA 01

METHODS 02

03 ANALYSIS and RESULTS

04 CONCLUSIONS

DATA ①

Geomagnetic-Activity Parameters

1. All geomagnetic-activity parameters (Ap, Dst, and scalar B), except the aa index, were taken from the OMNIWeb data base **(omniweb.gsfc.nasa.gov).** The aa index were taken from the International Service of Geomagnetic Indices data base **(ISGI:isgi.unistra.fr).**

Solar-Flare İndex

1. The solar-flare index (FI) data are taken from the Bogazici University, Kandilli Observatory website **(https://astronomi.boun.edu.tr/flare-index).**

- All monthly values are calculated by taking the average of the daily values over the months for the 1975-2020 time interval.

DATA ①

- Flare Index (FI) is a solar activity index that describe the total energy emitted by a flare. It was described by the formula ***FI = it,*** which was introduced by Kleczek (1952), in order to estimate the daily flare activity over a 24-hour period. In this formula, ***i*** represents the flare intensity measured in the ***Hα*** spectral line, whereas ***t*** stands for the duration of the flare in minutes. Calculated daily/monthly values are publicly available, provided by the Kandilli Observatory (astronomi.boun.edu.tr/flare-index) as well as by the National Geophysical Data Center (NGDC: www.ngdc.noaa.gov/stp/solar/solarflares.html).

- The aa index is a simple global geomagnetic-activity index introduced by Mayaud (1972). It is derived from the K indices from two approximately antipodal observatories located at ±50◦ latitude (Hartland in the United Kingdom and Camberra in Australia) and it measures the amplitude of global geomagnetic activity during 3-hour intervals. The data are available since 1868.

- The Disturbance Storm Time (Dst) index was proposed by Sugiura (1964) to measure the magnitude of magnetospheric currents that produce an axially symmetric disturbance field. Irregularities observed in the Dst index that have a negative sign and fluctuate within the −50 nT ≤ Dst < −30 nT range are called small storms, while those within the −100 nT ≤ Dst < −50 nT range are called moderate storms, −200 nT ≤ Dst < −100 nT fluctuations are called intense storms, and a Dst index below −250 nT defines big geomagnetic storms (Gonzalez, Tsurutani, and Clúa de Gonzalez, 1999).

DATA ①

- Ap index: the K index is used to measure changes in the horizontal component of the magnetic field. However, since the K index is not directly related to geomagnetic activity the Kp index was introduced and it is derived from the mean standardized K index of 13 geomagnetic observatories located between ±44 and 60 degrees of the geomagnetic latitude. This planetary index is designed to measure the geomagnetic effect of solar particle radiation. The 3-hourly ap index is derived from the Kp index and the Ap index used in this study is an average of the ap index over 24 hours (Bartels, Heck, and Johnston, 1939).

- The interplanetary magnetic field (IMF) includes solar magnetic fields that were carried into interplanetary space by the solar wind. The source of the fast solar wind is thought to be coronal holes, which are open magnetic-field regions on the Sun, while slow solar wind originates at closed magnetic regions thought to be associated with active regions. The structure and dynamics of the IMF (scalar B) are key for understanding space weather (Owens and Forsyth, 2013).

METHODS ②

- We compared monthly averaged FI data with selected monthly averaged geomagnetic activity parameters for Cycles 21 to 24 (from 1976 to 2019).
- To investigate the relationship between FI and the selected geomagnetic parameters we first produced plots of their time variations.
- Then, the cross correlation analysis was performed and highest correlation coefficients between FI and the other indices were obtained along with the corresponding time lags.
- To examine periodic variations of all data sets used in this study the Morlet wavelet analysis method were performed. To see the details of periodic variations obtained by Morlet wavelet analysis of each monthly time series the Multi Taper Method (MTM) analysis were applied.
- To obtained the possible relationship between periodicities of FI and other indices (Ap, Dst, Scalar B (IMF), and aa) the “crosswavelet transform” (XWT) and the “wavelet coherence” (WTC) analysis methods were performed by using the biwavelet package written in R programming language (github.com/tgouhier/biwavelet).

ANALYSIS and RESULTS ③

1. Temporal Variation and Correlation Analyses

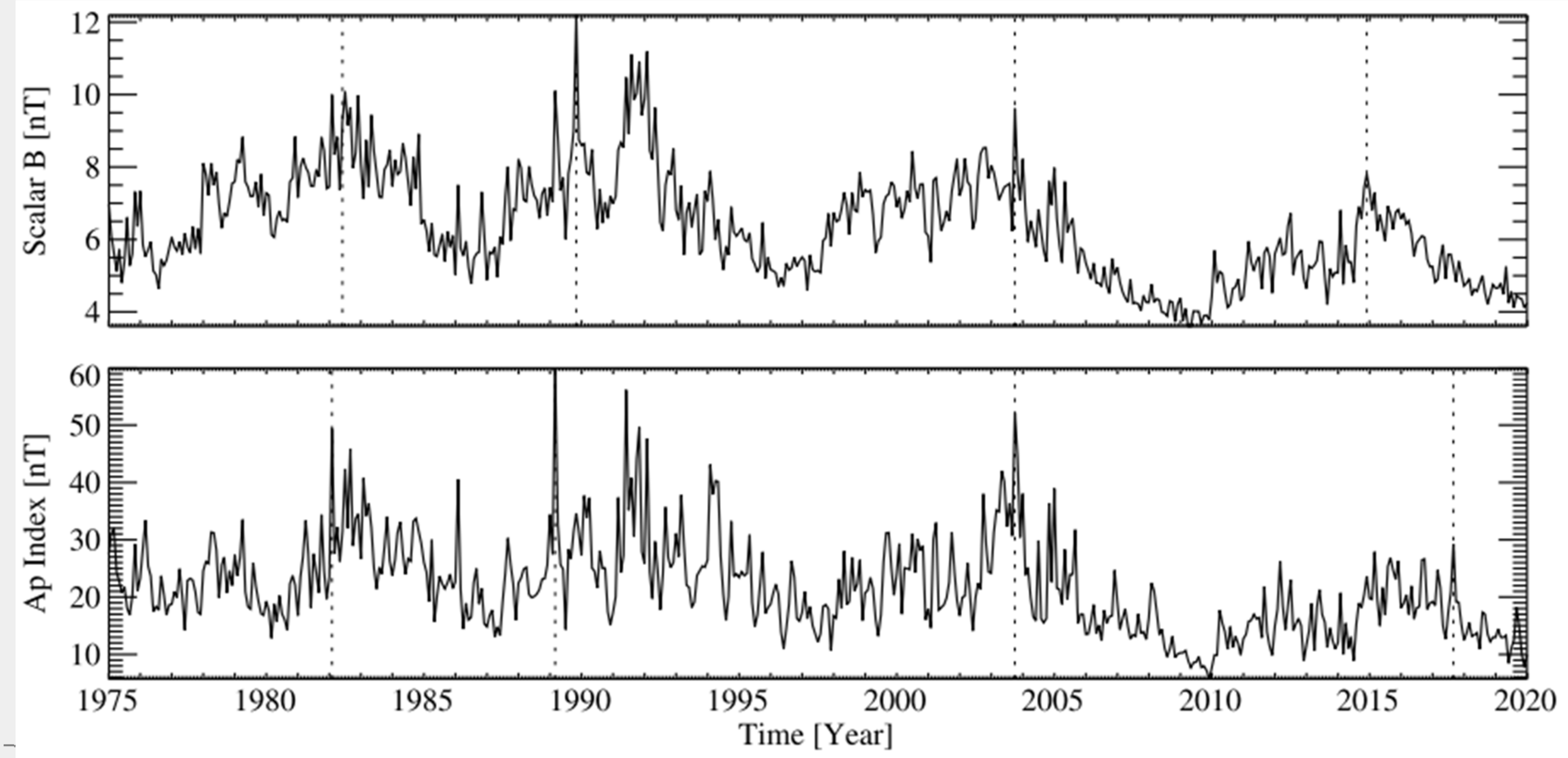

Figure 1. Temporal variations of investigated parameters for the time period of 1975 – 2020. The vertical dashed lines represent the peak position of each parameter for each cycle.

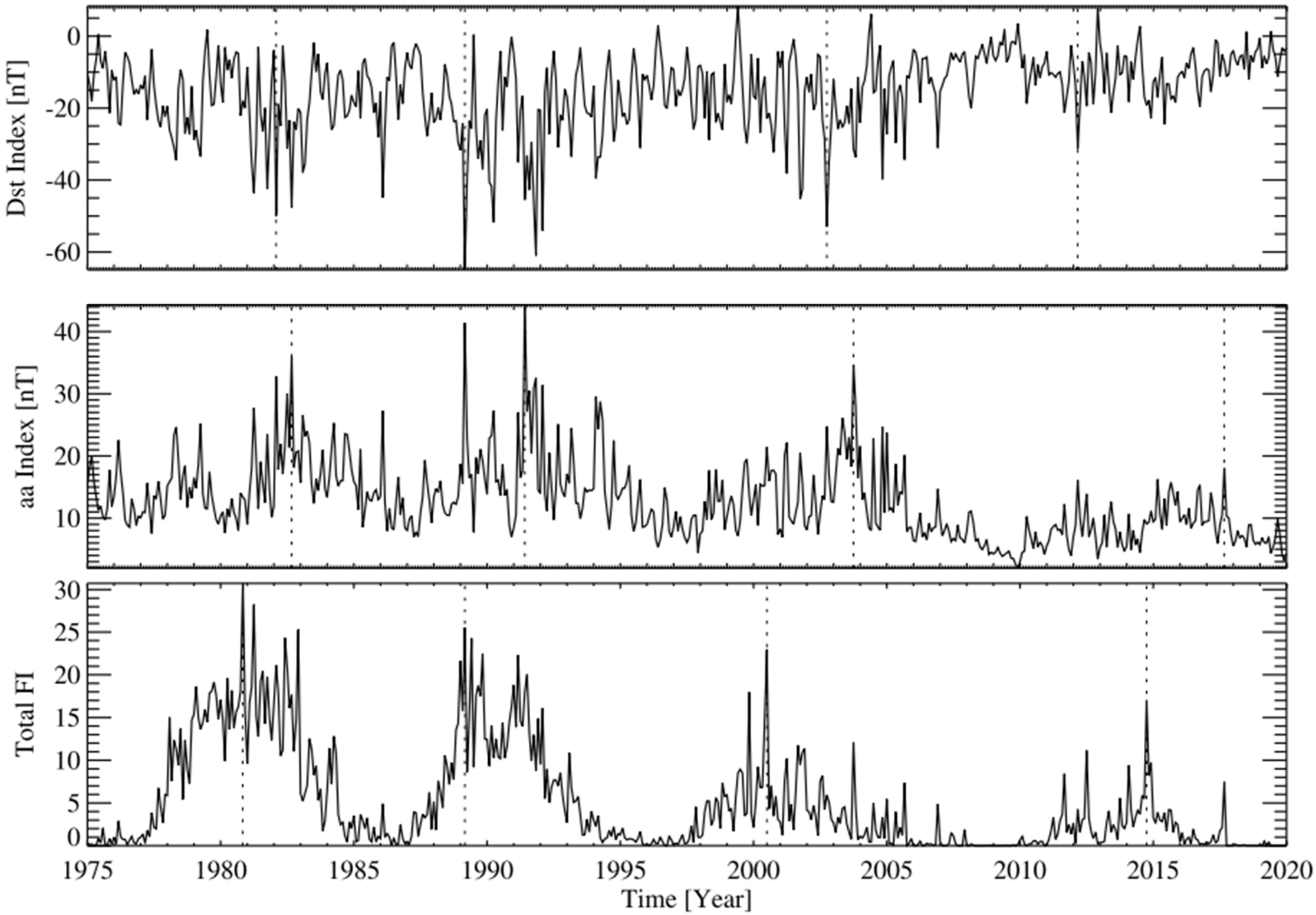

Dst Index [nT]
0
-20
-40
-60
aa Index [nT]
40
30
20
10
Total FI
30
25
20
15
10
5
0
1975
1980
1985
1990
1995
2000
2005
2010
2015
2020
Time [Year]

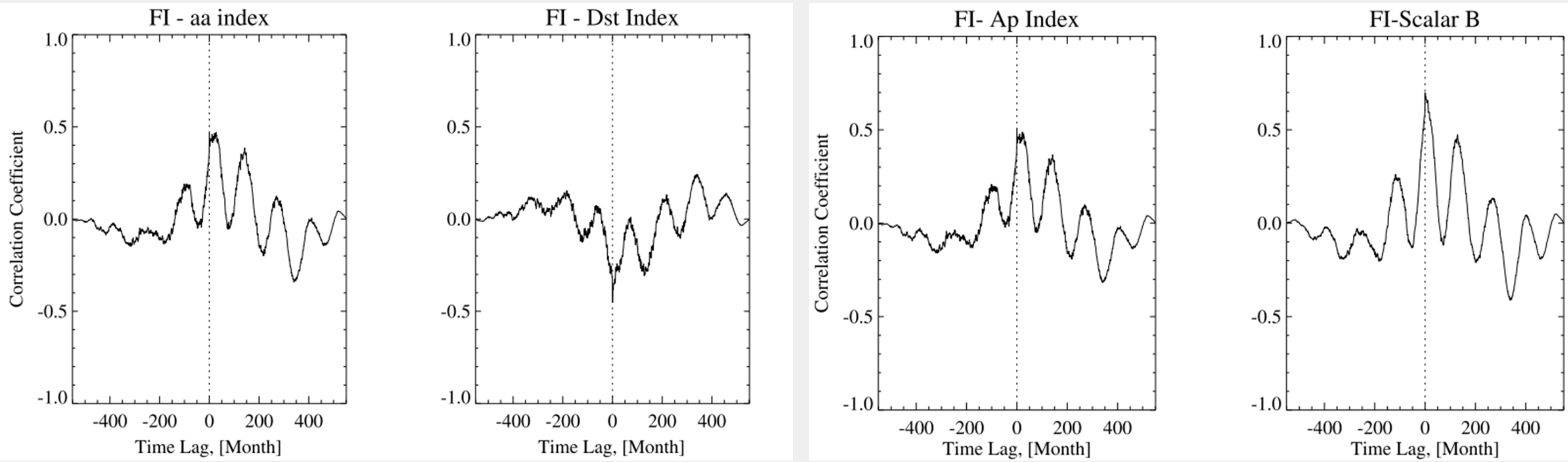

Figure 2. Cross-correlation analysis results for the investigated parameters. The vertical dotted lines show the zero-time lag.

Table 1. The maximum amplitudes of all used parameters for the investigated solar cycles.

Data	Cycle 21	Cycle 22	Cycle 23	Cycle 24
FI Index	30.73	25.53	22.94	17.01
Ap Index	49.35	60.04	52.24	29.27
Dst Index	−49.96	−64.97	−53.00	−31.19
aa Index	35.93	44.33	34.68	18.07
Scalar B	10.09	12.20	9.62	7.80

Table 2. Correlation coefficients and time lags between the monthly FI and geomagnetic-activity

Data	aa Index		Dst Index		Ap Index		Scalar B	
	Correlation coefficient	Lag [Month]	Correlation coefficient	Lag [Month]	Correlation coefficient	Lag [Month]	Correlation coefficient	Lag [Month]
Flare index	0.47 ± 0.07	27	-0.45 ± 0.07	0	0.51 ± 0.06	0	0.70 ± 0.05	0

2. Periodicity Analysis

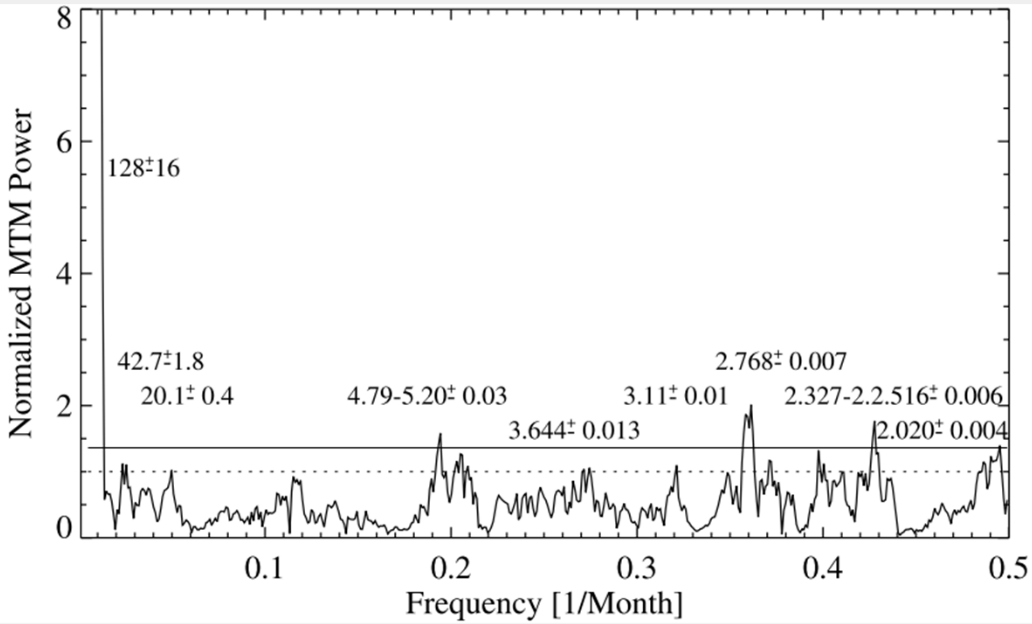

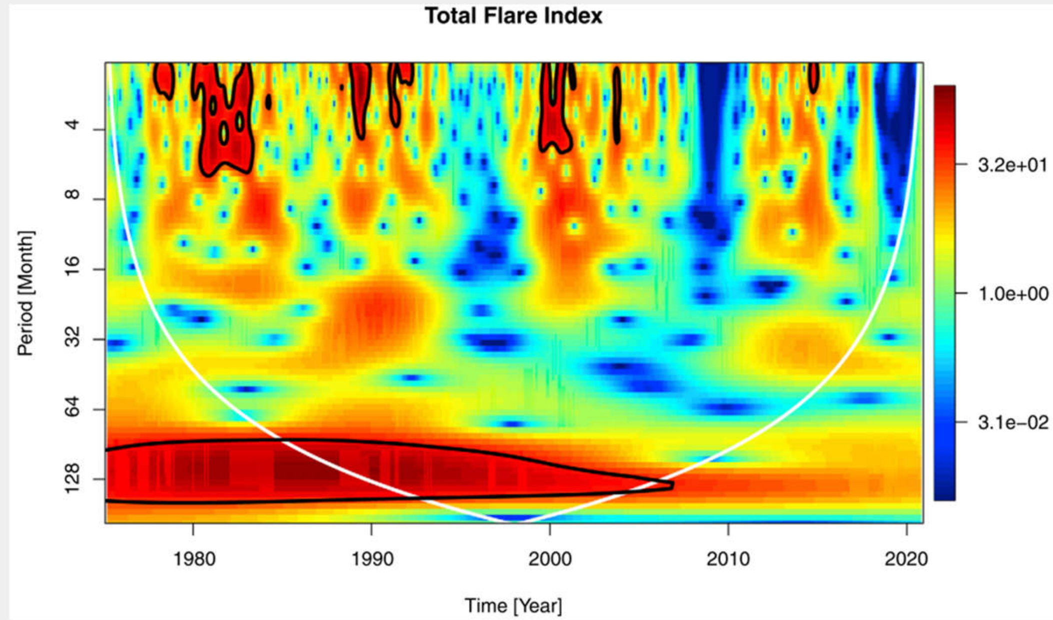

Figure 3. Results from MTM (left panel) and Morlet wavelet (right panel) analyses applied to FI data. Dashed and solid lines in the MTM spectrum represent 95% and 99% confidence levels, and the white line in the Morlet wavelet spectrum describes the cone of influence.

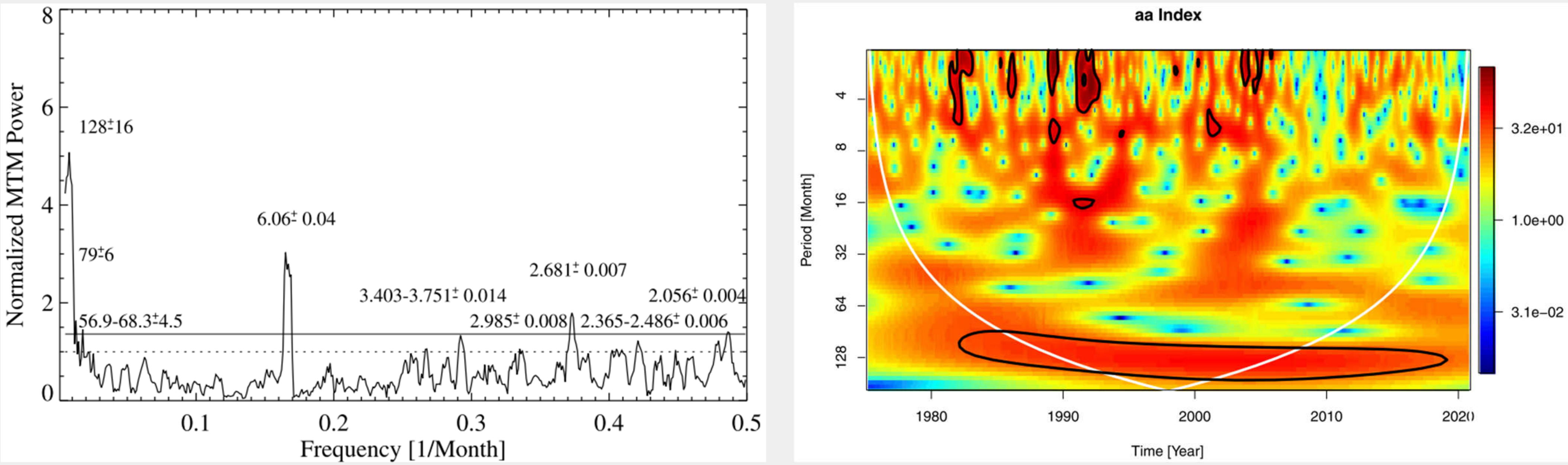

Figure 4. Results from MTM (left panel) and Morlet wavelet (right panel) analyses applied to the aa-index data. Dashed and solid lines in the MTM spectrum represent 95% and 99% confidence levels, and the white line in the Morlet wavelet spectrum describes the cone of influence.

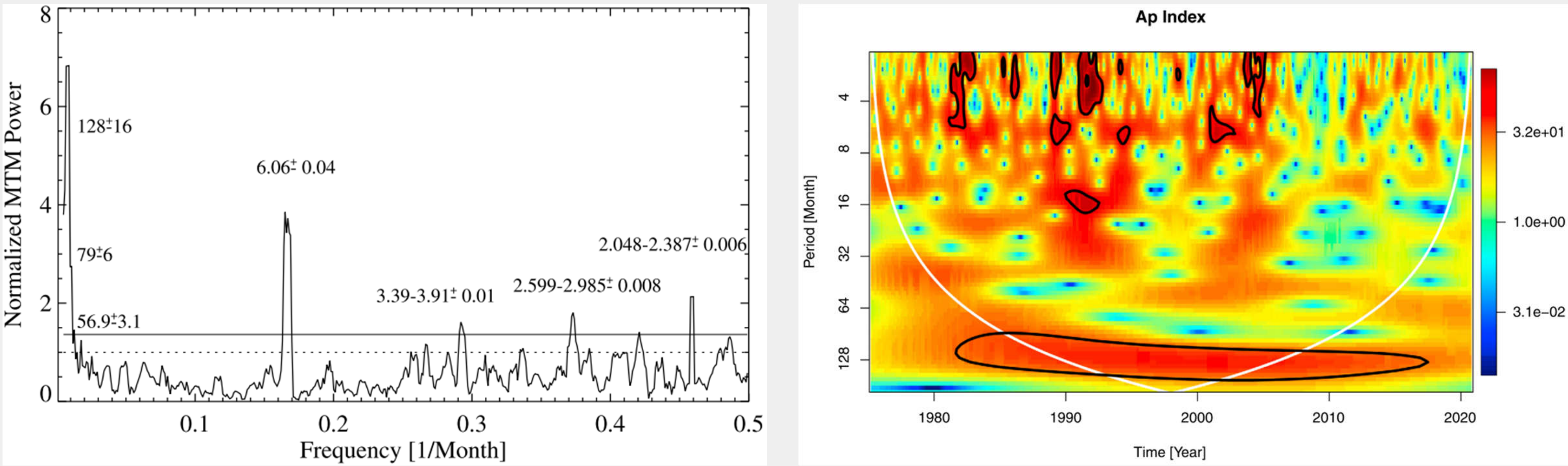

Figure 5. Results from MTM (left panel) and Morlet wavelet (right panel) analyses applied to the Ap index data. Dashed and solid lines in the MTM spectrum represent 95% and 99% confidence levels, and the white line in the Morlet wavelet spectrum describes the cone of influence.

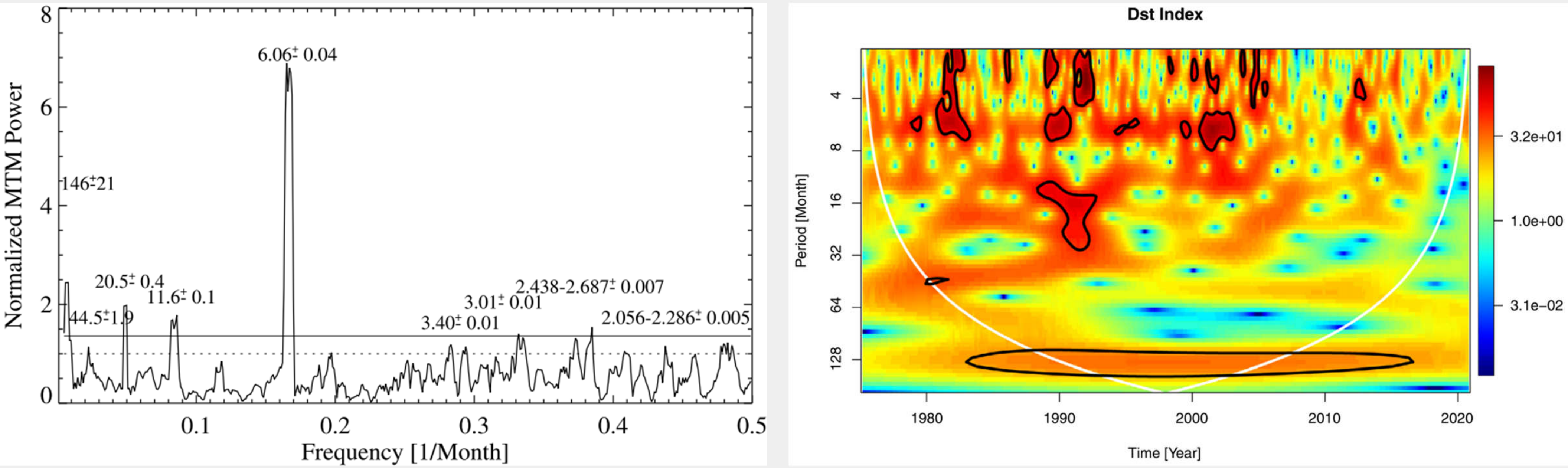

Figure 6. Results from MTM (left panel) and Morlet wavelet (right panel) analyses applied to the Dst index data. Dotted and dashed lines in the MTM spectrum represent 95% and 99% confidence levels, and the white line in the Morlet wavelet spectrum describes the cone of influence.

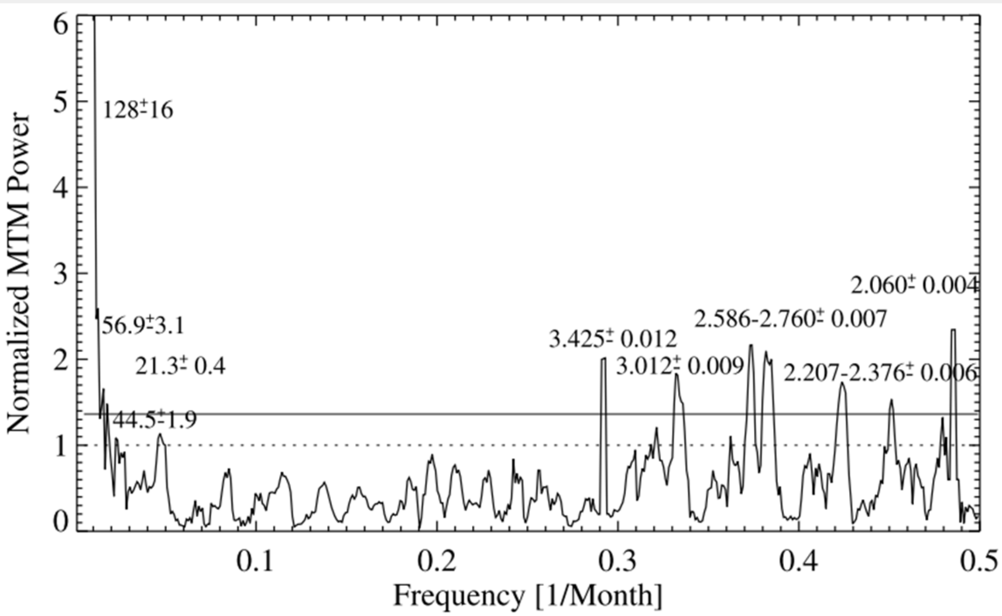

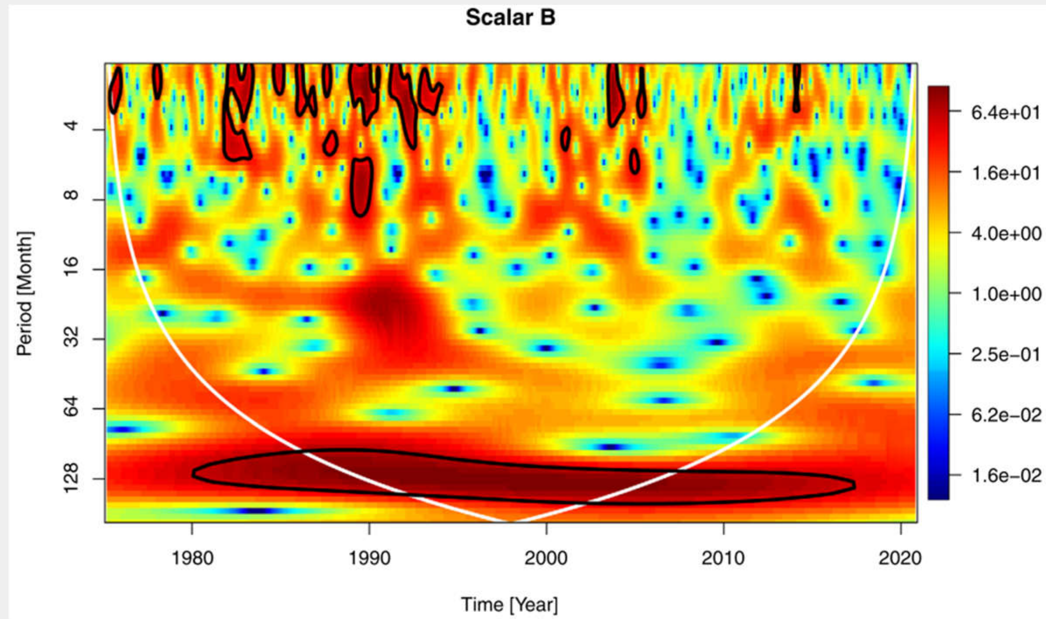

Figure 7. Results from MTM (left panel) and Morlet wavelet (right panel) analyses applied to the scalar B data. Dashed and solid lines in the MTM spectrum represent 95% and 99% confidence levels, and the white line in the Morlet wavelet spectrum describes the cone of influence.

Table 3. Periods detected with the MTM analysis and their significance level.

Period (Month)	FI	aa Index (nT)	Ap Index (nT)	Dst Index (nT)	Scalar B (nT)
114 – 128	+ > 99%	+ > 99%	+ > 99%	+ > 99%	+ > 99%
78 – 79	–	+ > 99%	+ > 99%	–	–
57 – 68	–	+ > 99%	+ > 95%	–	+ > 99%
42 – 45	+ > 95%	–	–	+ > 99%	+ > 99%
20 – 22	+ > 95%	–	–	+ > 99%	+ > 95%
6.0 – 6.1	–	+ > 99%	+ > 99%	+ > 99%	–
4.8 – 5.2	+ > 95%	–	–	–	–
3.3 – 3.9	+ > 95%	+ > 95%	+ > 95%	+ > 95%	+ > 99%
2.5 – 3.1	+ > 95%	+ > 95%	+ > 95%	+ > 95%	+ > 99%
2.2 – 2.4	+ > 99%	+ > 95%	+ > 95%	+ > 95%	+ > 99%
2.0 – 2.19	+ > 95%	+ > 95%	+ > 95%	+ > 95%	+ > 99%

Crosswavelet Transform" (XWT) and "Wavelet Coherence" (WTC) analysis methods
allow us to infer a nonlinear relationship and common periods between two analyzed data sets, X and Y.

The XWT spectrum shows the phase relationship that is represented by arrows with the following convention: pointing right, in-phase; pointing left, antiphase; pointing straight up, the second series Y leads by 90◦; pointing straight down, the first series X leads by 90◦. The case when the arrows are distributed randomly indicates phase mixing between X and Y.

The WTC spectrum indicates the amount of common power between two time series as a function of time and frequency by computing the cross-correlation between the two time series

Here, we compared the total FI data with each of the other indices used in this study.

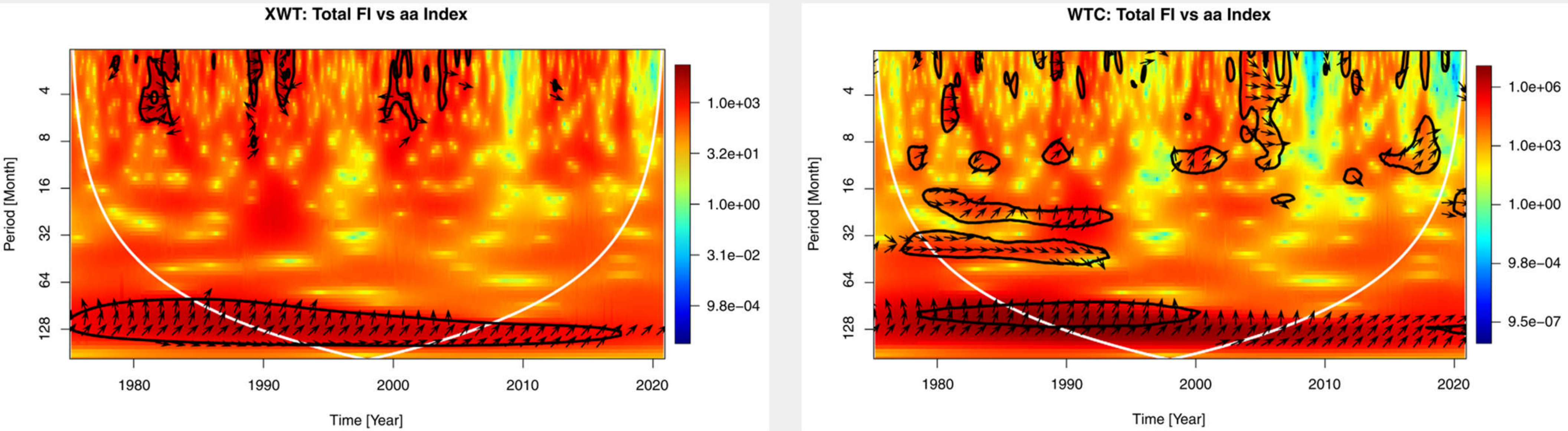

Figure 8. XWT (left panel) and WTC (right panel) spectrum between monthly FI and aa index.

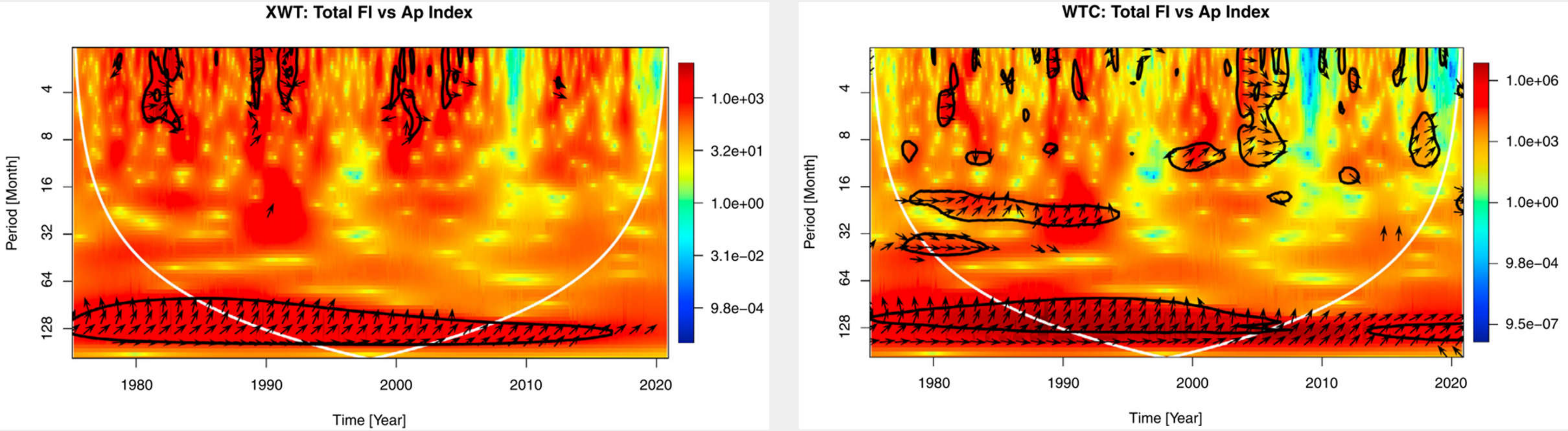

Figure 9. XWT (left panel) and WTC (right panel) spectrum between FI and Ap index.

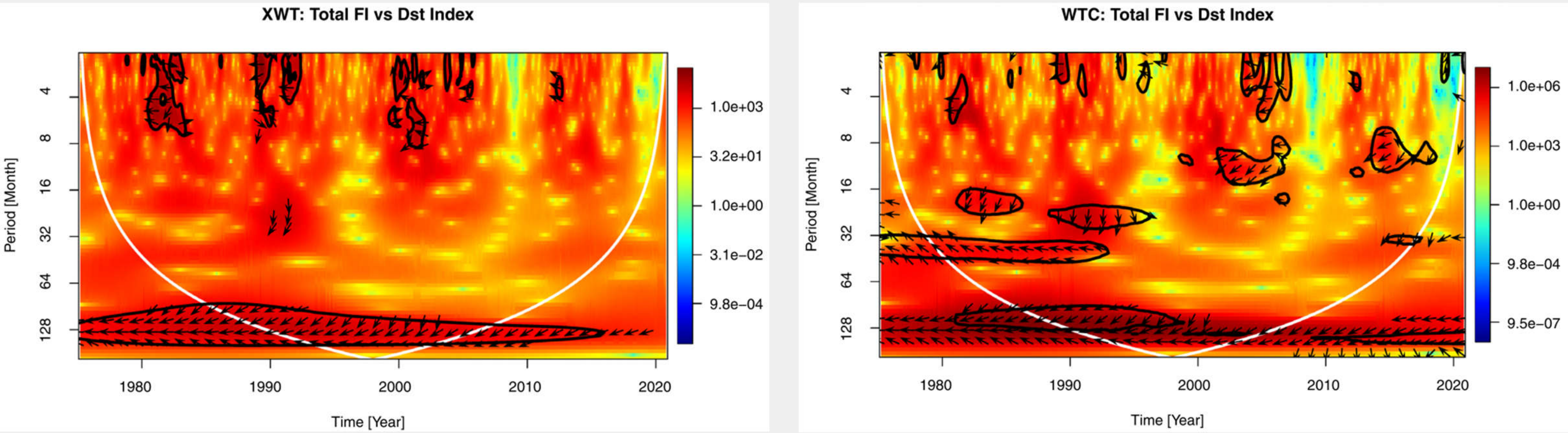

Figure 10. XWT (left panel) and WTC (right panel) spectrum between FI and Dst index.

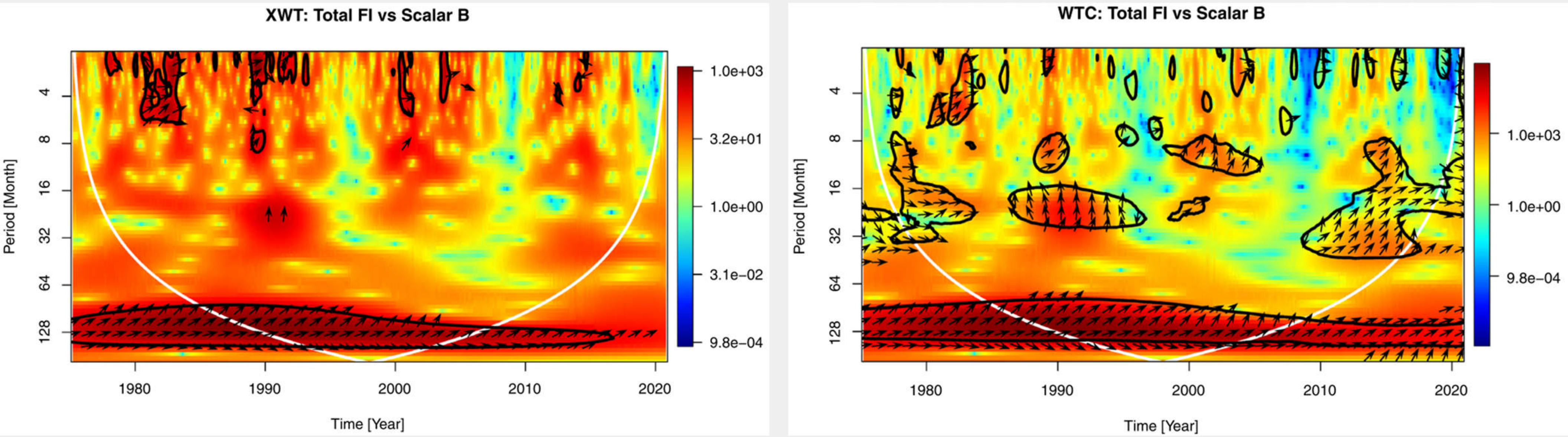

Figure 11. XWT (left panel) and WTC (right panel) spectrum between FI and scalar B.

CONCLUSIONS ④

In this study, we analyzed the relationship between FI and selected geomagnetic-activity parameters (aa, Ap, Dst, and scalar B) over four decades, 1976 – 2020 (four full solar cycles), on both global and regional scales. We focused on the temporal evolution of the employed solar FI and geomagnetic-activity parameters and quantified the correlation between them. Furthermore, MTM, Morlet wavelet, XWT, and WTC analysis techniques were used for the periodicity analyses of the investigated data sets.
The results of our analysis are as following:

1. The temporal variations of the used data sets show some differences; all data sets except FI peak values gradually decreased after 1992; the FI data peak value gradually decreased since 1982 (see Figure 1 and Table 1).
2. All data sets show double or multiple peaks during the maximum phase of the investigated solar-cycle maxima.
3. FI shows the highest correlation with scalar B ($r = 0.69 \pm 0.05$), while it shows the lowest correlation with the Dst index ($r = -0.45 \pm 0.07$) with zero-time lag. Only the geomagnetic aa index shows about a 27-month time lag with the FI data set.

4. About 11-year sunspot cycle periodicity and periodicities lower than 3.9 months are observed in all data sets without any exception. All periodicities were observed during the maximum phases of the Solar Cycles 21 – 23, while only a few periodicities were observed during Solar Cycle 24.
5. FI data have one special period interval (4.8 – 5.2 months) in which all other parameters do not show this periodicity, while geomagnetic aa, Ap, and Dst indices show 6 – 6.1-month periodicity and this period does not appear in the scalar B and FI data sets.
6. Geomagnetic aa and Ap indices have a coincident periodic behavior, while other data sets show some discrepancies.
7. XWT spectra between FI and other parameters generally show phase mixing in the small periods (2 – 8 months), while all parameters used in this study are in phase and highly correlated for the 11-year solar activity periodicity. Note that FI and Dst index data are in antiphase for the 11-year solar cycle periodicity.
8. In the WTC spectra, correlations are seriously decreasing for small periods for all data sets except for the declining phase of Solar Cycle 23. During this phase of Cycle 23 correlations between small periods seriously increased. Contrary to small periods, correlations for the 8- to 45-month periodicities increased during the investigated time interval (see right panels of Figures 8 to 11).

THANKS FOR YOUR ATTENTION